

B.P., as indicated by the earliest carbonized bone date, these new dates confirm that the site is chronologically more recent than Ganj Dareh by at least 500 years, and perhaps by as much as a millennium.

By resolving the temporal placement of these two sites, it is possible to place the initial domestication of goats in the highland Zagros region well within the natural habitat of this species. The long-term concentration on the hunting of wild goats in this upland region seen in assemblages stretching as far back as the Middle Paleolithic (2) suggests that the eventual domestication of goats grew out of a long-term process in which hunting strategies evolved into the actual management of captive animals. Ganj Dareh represents an early stage in herd management, in which the feeding, movement, and other environmental circumstances of these animals was little changed. Although the Ganj Dareh goats may not yet be morphologically, or even genetically, distinguishable from wild goats, however, the distinctive profile of young male slaughter and prolonged female survivorship documented here marks the goats of Ganj Dareh as a managed, and therefore domesticated, population.

The subsequent establishment some 500 to 1000 years later of settlements like Ali Kosh, outside this natural habitat zone, represents a break with the environmental, biological, and social context of initial domestication. This move seems to have necessitated some adjustments in management strategies from those developed in the upland zone. It also allowed the expression of morphological traits not widely seen in either wild or domesticated goats in upland habitats, such as the gradual alteration in the shape of horns identified by Flannery and, possibly, the reduction in the size of the Ali Kosh goats seen in this study.

Such morphological changes, if related to the process of domestication at all, are only delayed, and possibly indirect, artifacts of human management. Instead, it is the transformation of strategies that seek to maximize offtake from wild herds into those that seek to control the productivity of captive herds that lies at the heart of the process of animal domestication. The method for computing sex-specific age profiles developed here provides the most sensitive tool to date for monitoring this transformation and should be applicable not only to goats, but to any sexually dimorphic species. Combined with high-precision small-sample AMS dating, it promises a much finer understanding of the timing and trajectory of the origins of animal domestication across the Near East and beyond.

References and Notes

1. B. D. Smith, *The Emergence of Agriculture* (Freeman, New York, ed. 2, 1998); H. Pringle, *Science* **282**, 1446 (1998).

2. F. Hole, in *The Origins and Spread of Agriculture and Pastoralism in Eurasia*, D. Harris, Ed. (Smithsonian Press, Washington, DC, 1996), pp. 263–281.
3. H.-P. Uerpmann, *Probleme der Neolithisierung des Mittelmeerraumes* (no. 27, Dr Ludwig Reichert, Wiesbaden, Germany, 1979).
4. R. Meadow, in *The Walking Larder: Patterns of Domestication, Pastoralism, and Predation*, J. Clutton-Brock, Ed. (Unwin Hyman, London, 1989), pp. 80–90.
5. P. Ducos and L. R. Kolska Horwitz *Paléorient* **23**, 229 (1997).
6. B. Hesse, *Man* **17**, 403 (1982); in *Animals and Archaeology 3. Early Herders and Their Flocks*, J. Clutton-Brock and C. Grigson, Eds. (no. 202, British Archaeological Reports, London, 1984), pp. 243–264.
7. M. A. Zeder, *J. Archaeol. Sci.*, in press; *Paléorient*, in press.
8. B. Hesse, thesis, Columbia University (1978).
9. F. Hole, K. V. Flannery, J. Neely, *Prehistory and Human Ecology on the Deh Luran Plane* (Memoir no. 1, Museum of Anthropology, University of Michigan Press, Ann Arbor, MI, 1969).
10. O. Bar-Yosef and R. Meadow, in *Last Hunters, First Farmers: New Perspectives on the Transition to Agriculture*, D. Price and A.-B. Gebauer, Eds. (School of American Research, Santa Fe, NM, 1995), pp. 39–94.
11. S. Payne, *Anatolian Stud.* **23**, 281 (1973); R. W.

Redding, thesis, University of Michigan (1981). Ages of bone fusion, taken from I. A. Silver, in *Science and Archaeology*, D. Brothwell and E. Higgs, Eds. (Basic Books, New York, 1963), pp. 250–268. Silver's ages of fusion serve as a widely used standard but are likely too young for ancient populations.

12. F. Hole, in *Chronologies in the Near East*, O. Aurench, J. Evin, F. Hours, Eds. (no. 379, British Archaeological Reports, Oxford, 1987), pp. 353–379.
13. R. E. M. Hedges, R. A. Housley, C. R. Bronk, G. J. van Klinken, *Archaeometry* **32**, 231 (1990).
14. This more recent date for the initial occupation of Ali Kosh agrees with AMS dates of two charred bone samples from the same levels run by the Oxford Radiocarbon Accelerator Unit: OxA-1774, 7950 ± 110 ¹⁴C yr B.P.; and OxA-1773, 7830 ± 90 ¹⁴C yr B.P. (13).
15. Funded by a Smithsonian Predoctoral Fellowship awarded to B.H. in 1976, and by grants from the Smithsonian's Research Initiative and Scholarly Studies Programs awarded to M.A.Z. Acknowledgment is given to the staff of the Field Museum of Natural History; to A. Aisen, S. Arter, N. Cleghorn, M. Hiers, H. Lapham, S. McClure, C. McLinn, A. Shapiro, and S. Stackhouse; and to M. J. Blackman, B. D. Smith, P. Wapnish, and three anonymous reviewers.

3 November 1999; accepted 21 January 2000

Molecular Linkage Underlying Microtubule Orientation Toward Cortical Sites in Yeast

William S. Korinek, Matthew J. Copeland, Amitabha Chaudhuri, John Chant*

Selective microtubule orientation toward spatially defined cortical sites is critical to polarized cellular processes as diverse as axon outgrowth and T cell cytotoxicity. In yeast, oriented cytoplasmic microtubules align the mitotic spindle between mother and bud. The cortical marker protein Kar9 localizes to the bud tip and is required for the orientation of microtubules toward this region. Here, we show that Kar9 directs microtubule orientation by acting through Bim1, a conserved microtubule-binding protein. Bim1 homolog EB1 was originally identified through its interaction with adenomatous polyposis coli (APC) tumor suppressor, raising the possibility that an APC-EB1 linkage orients microtubules in higher cells.

The orientation of microtubules toward defined cortical sites in eukaryotic cells is a common theme in the regulation of nuclear position, the targeting of secretion, the navigation of growth cones, and the alignment of mitotic spindles. However, identification of the molecular means by which microtubules associate with spatially defined sites on the cortex has remained elusive. Budding yeast must align the mitotic spindle in parallel to the mother-bud axis to segregate one nucleus to each progeny cell. It is thought that cytoplasmic microtubules are selectively oriented toward the bud and that the forces generated by microtubule motors and microtubule

shortening produce the movement and alignment of the spindle (1–5). The budding yeast *KAR9* was genetically defined as being required for spindle alignment (6, 7), and the Kar9 protein localizes to the tips of buds and mating projections, two positions toward which microtubules become oriented (7). No microtubule binding has been shown for Kar9.

To determine the mechanism by which microtubules are oriented toward the bud tip in yeast, a two-hybrid screen was performed with Kar9. One interacting protein was Bim1, which was isolated in a two-hybrid screen against α -tubulin (BIM, binds to microtubules) (8). Bim1 exhibited strong and specific interactions with Kar9 (Fig. 1A). Although direct binding of Bim1 to microtubules has not yet been reported, Bim1 does associate with the microtubule cytoskeleton and affects microtubule dynamics in

Department of Molecular and Cellular Biology, Harvard University, 7 Divinity Avenue, Cambridge, MA 02138, USA.

*To whom correspondence should be addressed. E-mail: chant@fas.harvard.edu

REPORTS

yeast (8, 9). Bim1 may also be a component of a checkpoint pathway that monitors mitotic spindle alignment (10).

Specific binding was observed between a fusion protein made of glutathione S-transferase and Bim1 (GST-Bim1), which was purified from *Escherichia coli*, and Kar9 that was synthesized and radiolabeled in vitro (Fig. 1B). GST-Bim1 bound to radiolabeled Kar9 protein and showed no affinity for the control protein luciferase. A control fusion protein, GST-Hof1, showed no affinity for Kar9. In further experiments, a GST-Kar9 fusion protein bound to the epitope-tagged Bim1 in crude yeast extracts (Fig. 1C). Finally, GST-Kar9 and tagged Bim1 coprecipitated from extracts of yeast expressing both proteins (Fig. 1D).

Genetic evidence has suggested that spindle alignment in yeast is produced by two independent pathways: one defined by *KAR9* and the other defined by dynein and dynactin components. Because the path-

ways overlap in directing spindle alignment, the combination of mutations between pathways leads to a complete block in spindle alignment and to lethality (7, 11). When mutations affecting components of the same pathway are combined, the double-mutant phenotype is no more severe than either of the single-mutant phenotypes. Binding between Kar9 and Bim1 suggests that Bim1 is a component of the Kar9 pathway. Although *bim1* mutations are lethal in combination with mutations affecting the dynactin component (*act5*), this genetic interaction has been interpreted to indicate that Bim1 is part of a checkpoint that protects the cell from dividing prematurely if a defect in spindle alignment occurs (10). An alternative view is that Bim1 plays a mechanistic role in microtubule orientation and spindle alignment. This mechanistic role is consistent with the observations of Schwartz *et al.*, who reported that *bim1* mutants exhibit a microtubule orientation defect during mating, where cells are arrested in G₁ and a mitotic spindle checkpoint would be irrelevant (8). Although the two proposed roles for Bim1 are not mutually exclusive, if Bim1 is a com-

ponent of a general checkpoint that monitors spindle alignment, then *bim1* should be lethal in combination with *kar9*, a mutant that has a spindle alignment defect. Unlike the lethal *bim1act5* combination, the *bim1kar9* double mutant was viable and had a growth rate identical to that of the *bim1* or *kar9* single mutant (12). Analyzed quantitatively, the *bim1* and *kar9* mutants had similar defects in spindle movement and alignment, and importantly the phenotype of the *bim1kar9* double mutant was no more severe than the phenotypes of the single mutants (Fig. 2, A and B). In a control experiment, combining *kar9* with a mutation in *BIK1*, which has similar genetic properties to *bim1* and encodes a microtubule-binding protein (13), leads to a double-mutant phenotype which is enhanced in severity as compared to the phenotypes of the single mutants (7, 12). The finding that the *kar9* and *bim1* mutations are not additive in terms of phenotype suggests that their products act in the same pathway or work together as a complex.

Kar9 localizes to a cap at the distal tip of the bud and to cytoplasmic microtubules in yeast (7). Bim1 also localizes to microtu-

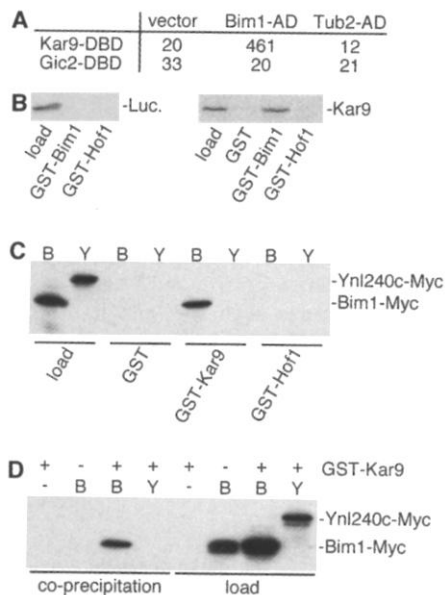


Fig. 1. Specific binding between Kar9 and Bim1. (A) Two-hybrid interaction between Kar9 fused to the Gal4 DNA binding domain (DBD) and Bim1 fused to the Gal4 activation domain (AD) were measured by standard methods (27). Numbers represent units of β -galactosidase activity. (B) GST-Bim1 precipitates Kar9 in vitro. Interactions between the indicated GST fusion proteins and Kar9 or luciferase were detected by autoradiography (28). (C) GST-Kar9 precipitates Bim1 from crude yeast lysates. Extracts from strains with either myc-tagged Bim1 or a myc-tagged control protein, Ynl240c, were incubated with GST, GST-Kar9, or GST-Hof1 (28). Myc-tagged proteins were detected by immunoblotting. B, myc-tagged Bim1; Y, myc-tagged control Ynl240c. (D) Kar9 and Bim1 coprecipitate in yeast extracts. Extracts of strains expressing GST-Kar9 and either myc-tagged Bim1 or myc-tagged Ynl240c were precipitated with glutathione sepharose beads and were immunoblotted with antibodies to myc (29).

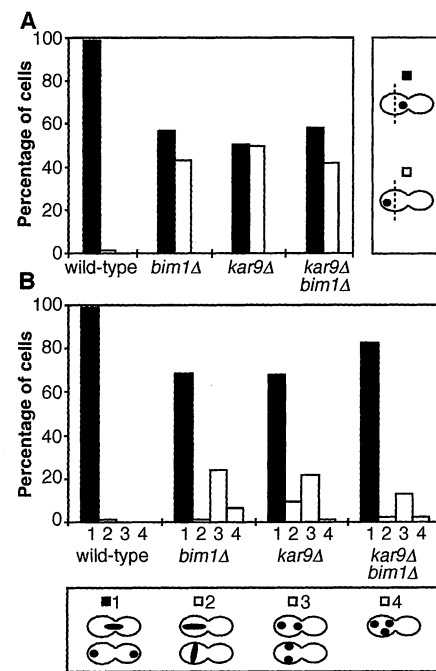


Fig. 2. *kar9* and *bim1* mutants show similar defects in spindle migration and alignment whereas double mutants show no enhancement in the severity of their phenotype. (A) Effects of *kar9* and *bim1* mutations on nuclear migration. In large budded cells, undivided nuclei were scored as being in the bud-proximal (solid bar) or bud-distal (open bar) hemisphere of the mother cell (30). (B) Large budded cells with elongated or divided nuclei were scored as to whether the nuclear or spindle alignment had (solid bar) or had not (open bar) occurred properly (30).

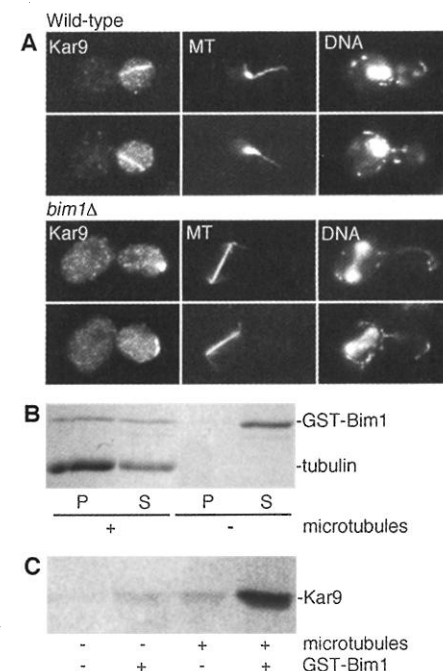


Fig. 3. The association of Kar9 with microtubules is dependent on Bim1 in vivo and in vitro. (A) Kar9-GFP, microtubules (MT), and DNA as seen in wild-type and *bim1* Δ cells (31). The association of Kar9 with microtubules, observed in wild-type cells, was abolished in a *bim1* mutant. (B) GST-Bim1 sediments (P) with microtubules in a standard microtubule pelleting assay, but remains in the supernatant (S) in the absence of microtubules (32). (C) Bim1 recruits Kar9 to microtubules. In vitro-translated Kar9 efficiently co-pellets with microtubules only when added in combination with Bim1 (32, 33).

bules with some preference for their distal ends (8, 9). When overexpressed, Kar9 was detected in association with cytoplasmic microtubules (Fig. 3A). This association was abolished in a *bim1*-null mutant. According to the view that Kar9 acts on microtubules through Bim1, Bim1 should be able to recruit Kar9 to microtubules in vitro. Kar9 did not readily associate with microtubules in vitro (Fig. 3, B and C). However, the addition of purified Bim1 promoted Kar9 co-sedimentation with microtubules. Thus, Kar9 appears to interact with cytoplasmic microtubules through Bim1.

Overexpression of *KAR9* often resulted in the aberrant translocation of the entire nucleus and spindle into the bud (Fig. 4). To test the view that Kar9 acts through Bim1, we examined the extent of this gain-of-function phenotype in a *bim1*-null mutant and a *bik1*-null control mutant. When *KAR9* was overexpressed, 28% of cells with large buds had nuclei translocated into the bud. The *bim1*-null mutation reversed this phenotype to a low level (2%), the same level of nuclear translocation observed before *KAR9* expression, while the *bik1*-null mutation had little effect (32%).

We propose the following mechanism by which microtubules are oriented toward the bud tip. The exploratory movements of individual microtubules search the cytoplasm for stabilization sites (3, 4, 14). When a growing microtubule extends into the bud, the interaction between cortical Kar9 and microtubule-bound Bim1 stabilizes the microtubule tip. Forces from motors and/or microtubule shortening act on this microtubule tether to align the spindle. Bim1 belongs to the EB1 family of microtubule-binding proteins. EB1

was identified through its binding to the adenomatous polyposis coli (APC) tumor suppressor protein, defects of which contribute to colon cancer (15–17). APC localizes to cortical sites associated with microtubule stabilization, supporting the possibility of a linkage analogous to Kar9-Bim1 whereby APC acts through EB1 to orient microtubules to spatially defined cortical sites (18).

References and Notes

1. J. V. Kilmartin and A. E. Adams, *J. Cell Biol.* **98**, 922 (1984).
2. M. Snyder, S. Gehrung, B. D. Page, *J. Cell Biol.* **114**, 515 (1991).
3. J. L. Carminati and T. Stearns, *J. Cell Biol.* **138**, 629 (1997).
4. S. L. Shaw, E. Yeh, P. Maddox, E. D. Salmon, K. Bloom, *J. Cell Biol.* **139**, 985 (1997).
5. T. Stearns, *J. Cell Biol.* **138**, 957 (1997).
6. L. J. Kurihara, C. T. Beh, M. Latterich, R. Schekman, M. D. Rose, *J. Cell Biol.* **126**, 911 (1994).
7. R. K. Miller and M. D. Rose, *J. Cell Biol.* **140**, 377 (1998).
8. K. Schwartz, K. Richards, D. Botstein, *Mol. Biol. Cell* **8**, 2677 (1997).
9. J. S. Tirnauer, E. O'Toole, L. Berrueta, B. E. Bierer, D. Pellman, *J. Cell Biol.* **145**, 993 (1999).
10. L. Muhua, N. R. Adams, M. D. Murphy, C. R. Shields, J. A. Cooper, *Nature* **393**, 487 (1998).
11. R. K. Miller et al., *Mol. Biol. Cell* **9**, 2051 (1998).
12. W. S. Korinek, M. J. Copeland, J. Chant, unpublished data.
13. V. Berlin, C. A. Styles, G. R. Fink, *J. Cell Biol.* **111**, 2573 (1990).
14. T. Mitchison and M. Kirschner, *Nature* **312**, 237 (1984).
15. L. K. Su et al., *Cancer Res.* **55**, 2972 (1995).
16. J. Groden et al., *Cell* **66**, 589 (1991).
17. K. W. Kinzler et al., *Science* **253**, 661 (1991).
18. I. S. Nathke, C. L. Adams, P. Polakis, J. H. Sellin, W. J. Nelson, *J. Cell Biol.* **134**, 165 (1996).
19. P. James, J. Halladay, E. A. Craig, *Genetics* **144**, 1425 (1996).
20. J. H. Miller, *Experiments in Molecular Genetics* (Cold Spring Harbor Laboratory Press, Cold Spring Harbor, NY, 1972), pp. 352–355.
21. R. A. Sia, E. S. Bardes, D. J. Lew, *EMBO J.* **17**, 6678 (1998).
22. J. R. Pringle, A. E. Adams, D. G. Drubin, B. K. Haarer, *Methods Enzymol.* **194**, 565 (1991).
23. B. L. Goode and S. C. Feinstein, *J. Cell Biol.* **124**, 769 (1994).
24. M. S. Longtine et al., *Yeast* **14**, 953 (1998).
25. J. Sambrook, E. F. Fritsch, T. Maniatis, *Molecular Cloning: A Laboratory Manual* (Cold Spring Harbor Laboratory Press, Cold Spring Harbor, NY, ed. 2, 1989).
26. C. Kaiser, S. Michaelis, A. Mitchell, *Methods in Yeast Genetics: A Cold Spring Harbor Laboratory Course Manual* (Cold Spring Harbor Laboratory Press, Cold Spring Harbor, NY, 1994).
27. Strain PJ69-4A (19) carrying *KAR9-DBD* or *GIC2-DBD* was transformed with *BIM1-AD*, *TUB2-AD*, or the *AD* vector, and β -galactosidase units were measured (20). *KAR9-DBD*, pBK154; *GIC2-DBD*, pBK153; *BIM1-AD*, pBK155; *TUB2-AD*, pBK37; *AD* vector, pGAD-C2. β -galactosidase activity is an average of four independent runs.
28. GST and GST-fusion proteins were expressed in *E. coli* cells and purified with glutathione sepharose 4B beads (Pharmacia Biotech, Piscataway, NJ). All GST fusion proteins were made with the full-length protein stated except for Hof1, which was made with amino acids 1 through 286. GST, pGEX-4T-1; GST-Bim1, pBK141; GST-Hof1, pBK40; GST-Kar9, pBK140. In vitro translation used TNT Quick-Coupled Transcription/Translation Reticulocyte Lysate System (Promega). Kar9, pBK137; luciferase, luciferase T7 control DNA (Promega). Preparation of crude yeast lysates was essentially as described in Sia et al. (21). Bim1-Myc, BK514; Ynl240c-Myc, BK104. Labeled proteins and GST-fusions were in-

cubated for 2 hours at 4°C. The beads were washed five times with buffer B [20 mM tris-HCl (pH 7.5), 0.2% NP-40, 0.25% bovine serum albumin (BSA)], including either 150 mM NaCl (Fig. 1B) or 500 mM NaCl (Fig. 1C).

29. Cultures for coprecipitations were incubated with galactose for 5 hours to induce GST-Kar9 and lysates were prepared as described above. The lysates were incubated with glutathione sepharose beads for 2 hours at 4°C and washed five times with buffer B containing 150 mM NaCl. An immunoblot was prepared and probed with 9E10 mouse monoclonal antibody to myc (Berkeley Antibody, Richmond, CA), horseradish peroxidase-conjugated goat secondary antibody to mouse antibody (Jackson Immunologicals, Westgrove, PA), and visualized with SuperSignal chemiluminescence (Pierce, Rockford, IL). *GST-KAR9*, BK511; *BIM1-MYC*, BK514; *GST-KAR9 BIM1-MYC*, BK572; *GST-KAR9 YNL240c-MYC*, BK574.
30. *bim1kar9* double mutants were isolated by meiotic tetrad analysis, and genotypes were confirmed by polymerase chain reaction (PCR). Log phase cells were fixed and stained with Hoechst 33342 (Molecular Probes, Eugene, OR). Two independent counts were performed on each strain. The average of the four counts is shown, each $n > 300$ cells. Wild-type, BK536 and BK537; *kar9Δ*, BK534 and BK538; *bim1Δ*, BK533 and BK539; *kar9Δ bim1Δ*, BK535 and BK540.
31. Standard yeast immunofluorescence techniques were used (22). Kar9-green fluorescence protein (Kar9-GFP) was induced from the *MET25* promoter (pBK115) for either 2 (Fig. 3A) or 4 hours (Fig. 4) prior to fixing with 3% formaldehyde. Kar9-GFP was visualized with polyclonal rabbit antibody to GFP and CY3-conjugated secondary antibody rabbit immunoglobulin G (IgG) (Jackson Immunologicals). Microtubules were visualized with monoclonal rat antibody to YOL1/34 (Accurate Chemical, Westbury, NY) and fluorescein isothiocyanate-conjugated secondary antibody to rat IgG (Jackson Immunologicals). DNA was stained with Hoechst 33342 (Molecular Probes). Wild-type, SEY6210; *bim1Δ*, BK529; *bik1Δ*, BK543.
32. An in vitro microtubule affinity assay was performed essentially as described by Goode and Feinstein (23) with the following notes. Bovine brain tubulin protein (Cytoskeleton, Denver, CO) was polymerized for 20 min at 35°C and stabilized with 20 μ M taxol (Cytoskeleton). Polymerized tubulin (50 to 100 μ g) was incubated with test proteins for 20 min. Reactions were then loaded into 800- μ l Ultra Clear centrifuge tubes (Beckman) over 550 μ l of a glycerol cushion buffer (30% glycerol, 1 mM guanosine triphosphate, 80 mM Na-Pipes (pH 6.9), 1 mM MgCl₂, 1 mM EGTA) (Cytoskeleton) and were supplemented with 20 μ M taxol. In addition to about 10 ng of in vitro-translated Kar9, 100 ng of purified GST-Bim1, and/or 5 μ g microtubules, reactions in Fig. 3C also contained 1 μ g of BSA (New England Biolabs, Beverly, MA) and 100 ng of His₆-tagged Kar9 protein (pBK161).
33. Yeast strains, plasmids, and DNA primers used in this study are listed in table 1 in the supplementary data, which is available at www.sciencemag.org/feature/data/1047752.shl. Gene deletions were made in an isogenic background and confirmed by PCR (24). Standard media, genetic methods, and DNA manipulations were used (25, 26). Yeast cultures were grown at 30°C and were in exponential phase at time of experiments.
34. We are grateful to members of the J. Chant laboratory and to K. Kaplan for helpful discussions and insight. We thank R. Losick for critically reading the manuscript, T. Chen for performing some supporting experiments, Y. Ho for the tagged *YNL240c* control, and J. Kahana and P. Silver for the antibodies to GFP. Supported by NIH grant GM49782 (J.C.) and grants GM07620-19 through GM07620-21 from an Institutional National Research Service Award, Training Program in Genetics (W.S.K.).

7 December 1999; accepted 11 February 2000

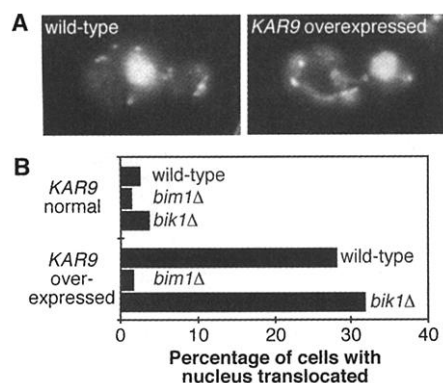


Fig. 4. Overexpression of *KAR9* leads to excessive nuclear migration, which is abolished by mutations in *BIM1*. (A) A wild-type cell is shown with its nucleus positioned at the mother-bud neck. A cell overexpressing *KAR9* is shown with the nucleus completely translocated into the bud. (B) The percentage of large budded cells with the nucleus completely translocated into the bud is shown in the indicated strains with or without *KAR9* overexpression. $n > 300$ cells (31, 33).